JOURNAL OF MATERIALS SCIENCE 28 (1993) 3059–3068

Si–C–N ceramics with a high microstructural stability elaborated from the pyrolysis of new polycarbosilazane precursors

Part V *Oxidation kinetics of model filaments*

D. MOCAER, G. CHOLLON, R. PAILLER, L. FILIPUZZI, R. NASLAIN
Laboratoire des Composites Thermostructuraux (UMR 47 CNRS-SEP-UB1), Domaine Universitaire, 3 Allée de La Boëtie, F-33600 Pessac, France

Oxidation tests have been performed on model Si–C–N–O filaments prepared from a new polycarbosilazane (PCSZ) precursor, according to a spinning–oxygen-curing–pyrolysis procedure. Thermogravimetric analyses have been run under a flowing atmosphere of dry oxygen ($P = 100$ kPa) at $1000 < T < 1400$ °C. The oxidation treatment results in the growth of a silica layer (passive oxidation regime) and simultaneously the release of carbon oxides and nitrogen, with an overall weight increase. At a given test temperature, the kinetics of growth of the silica scale obeys a parabolic law. The parabolic rate constant is thermally activated with an apparent activation energy of 170 kJ mol^{-1}. The rate-limiting step is diffusion-controlled. The ex-PCSZ filaments exhibit a better oxidation resistance than the related Si–C–O fibres prepared from polycarbosilane precursors according to a similar procedure.

1. Introduction

A number of Si-based ceramic fibres have been elaborated according to a spinning–stabilization–pyrolysis general procedure from various organosilicon precursors including polycarbosilanes (PCS) [1, 2], polytitanocarbosilanes (PTCS) [3, 4] and polysilazanes (PSZ) [5, 6]. These fibres were designed to be used in ceramic-matrix composites (CMCs) or metal-matrix composites (MMCs) at high temperatures and under oxidizing atmospheres [7–10]. The organosilicon precursors are usually spun in the molten state, so the green fibres have to be properly stabilized before the high-temperature pyrolysis. This is often done through a curing step with oxygen. Since the Si–O bonds are very stable, the oxygen which has been introduced in the material is not released during pyrolysis and remains in the fibres (with a weight concentration of the order of 10%). When such fibres are further aged in an inert atmosphere at high temperatures (i.e. $T > 1200$ °C), most of them undergo a decomposition–crystallization process with a drop in their mechanical properties. Now it is well established that this process involves the formation of gaseous oxides (i.e. SiO and CO) [11, 12]. Thus, improving the thermal stability of ex-organosilicon fibres through the use of new precursors and curing agents is a subject of active research [13, 14].

Surprisingly, very few articles have been devoted to the kinetics of oxidation of ex-organosilicon ceramic fibres despite the fact that most related MMCs or CMCs are used in oxidizing atmospheres. Warren and Anderson [15] and more recently Filipuzzi and Naslain [16] have studied the oxidation of ex-PCS Si–C–O fibres (Nicalon fibres from Nippon Carbon). The latter have shown that such fibres undergo a parabolic weight increase versus time, within the temperature range 850–1200°C. They assigned this feature to diffusion phenomena across the protective silica film formed on the fibre surface and reported an apparent activation energy value (i.e. ~70 kJ mol^{-1}) much lower than that usually accepted for pure polycrystalline SiC (i.e. ~200–300 kJ mol^{-1}). They also mentioned that beyond 1200 °C the kinetic data no longer obeyed parabolic laws owing to crystallization of the glassy silica film, the occurrence of microcracking and the intrinsic lack of stability of the fibres at high temperatures.

As far as we know, no detailed study has been published on the oxidation kinetics of ex-polysilazane and ex-polycarbosilazane (PCSZ) fibres. The aim of the present contribution is to report the oxidation kinetic data that we have obtained on model Si–C–N–O monofilaments prepared from new oxygen-cured PCSZ precursors according to a procedure which has been described elsewhere [17,18], and to compare the related kinetic law with those previously published for ex-PCS Si–C–O fibres [16] in order to try to point out the influence of the nitrogen atoms.

2. Experimental procedure

The PCSZ-precursor used in the present study was prepared according to a co-polymerization process,

0022–2461 ·

from dimethyldichlorosilane and 1,3-dichloro-1, 3-dimethyldisilazane, according to a procedure which has been described elsewhere [19]. Its chemical composition corresponds to the overall formula $SiC_{1.22}N_{0.45}H_{4.2}O_{0.03}$ and was referred to as PCSZ-II in part I [20]. The precursor was spun in the molten state, with a laboratory-scale apparatus equipped with a single spinneret. The green continuous monofilament (25 μm in diameter) was cut into lengths of about 50 mm and cured under a flowing oxygen–nitrogen mixture ($P(O_2) = 50$ kPa, $P(N_2) = 50$ kPa, $Q = 1\,l\,h^{-1}$) at 190 °C (heating rate 5 °C h^{-1}, duration of isothermal plateau 1 h), according to a procedure described and discussed in part II [17]. Finally, the oxygen cured filaments were pyrolysed under flowing argon ($P = 100$ kPa, $Q = 1\,l\,h^{-1}$) up to a temperature $T_p = 1200$ °C (the filaments being maintained at T_p for 15 min), as described in part III [18]. After pyrolysis, the chemical composition of the filaments corresponds to the overall formula $Si_1C_{0.77}N_{0.39}O_{0.6}$ (with trace amounts of hydrogen) [18].

The oxidation kinetics of the ex-PCSZ-II Si–C–N–O filaments were studied by thermogravimetric analysis (TGA) (TAG 24 apparatus from Sétaram). The experiments were performed on samples of 50 mg set in a pure alumina crucible and heated up to a maximum temperature T_0 ranging from 1000 to 1400 °C (heating rate 30 °C min^{-1}, isothermal plateau of 3 h at T_0) under a flow of pure dry oxygen ($P = 100$ kPa, $Q = 1\,h^{-1}$) (oxygen grade N45 ($H_2O < 2$ p.p.m.) from Alphagaz).

After the oxidation test, the morphology of the oxide scale was studied by scanning electron microscopy (SEM) (Jeol 840 S). Its structure and local composition were assessed by transmission electron microscopy (TEM) with electron energy loss spectroscopy (EELS) (ELS 50 from Vacuum Generators).

3. Results

3.1. Kinetics of oxidation of the filaments in dry oxygen

The relative weight variations of the filaments ($\Delta m/m_0$) as a function of time during exposures in dry oxygen are shown in Fig. 1a for $1000 < T_0 < 1400$ °C and $0 < t < 12\,000$ s. Oxygen exposures lead to an overall weight increase of the sample whatever the value of the temperature, thought to be the result of a complex chemical reaction involving the oxidation of the combined silicon from the filament into silica (occurring with a weight increase) and the evolution of gaseous species, i.e. CO, CO_2 and N_2 (taking place with a weight loss), as discussed later in section 4. Furthermore, the variations of $(\Delta m/m_0)^2$ as a function of time (Fig. 1b) were observed to be linear, a feature suggesting that the oxidation kinetics obeyed a diffusion-controlled law, as is usually the case for silicon-based ceramics in the so-called passive oxidation regime (growth of a protective silica scale) [21].

The thickness of the silica scale was calculated from the $\Delta m/m_0$ data assuming that (i) the composition of the non-oxidized part of the filament remained constant during the oxidation treatment (as supported by

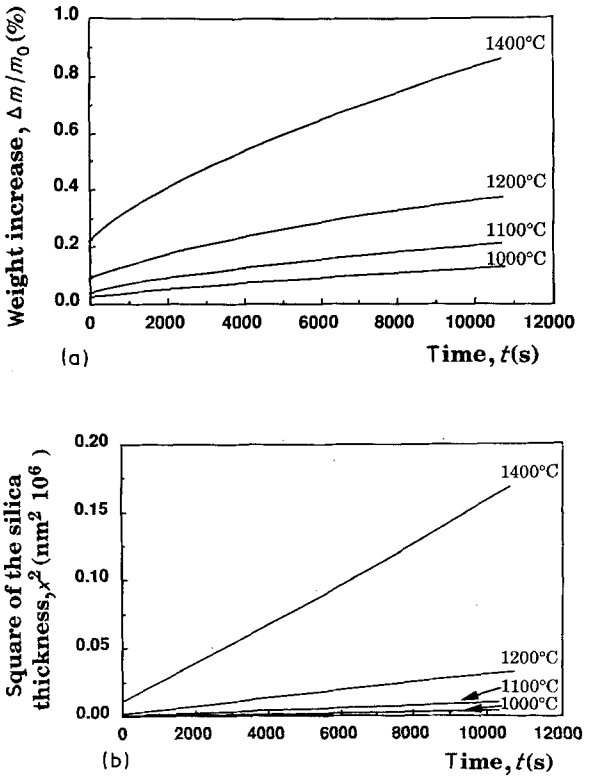

Figure 1 Oxidation kinetics of ex-PCSZ-II Si–C–N–O filaments in dry oxygen ($P = 100$ kPa, $Q = 1\,l\,h^{-1}$) at temperatures ranging from 1000 to 1400 °C: (a) variations of the weight increase of the sample $\Delta m/m_0$ versus time, (b) variations of the square of the mean thickness of the silica scale versus time.

electron-probe microanalysis data), (ii) the oxide scale is pure silica, the Si–C–N–O/SiO_2 conversion proceeding radially from the external filament surface, and (iii) the thickness of the silica layer is small comparatively to the fibre diameter. Under such assumptions and as established in the Appendix, the thickness of the silica layer x (expressed in nanometres) can be calculated from the value of $\Delta m/m_0$ according to the equation

$$\frac{x}{r} = F_R \frac{\Delta m}{m_0} \quad (1)$$

where F_R, the conversion factor, is equal to 0.044. This calculation procedure was validated on the basis of direct measurements of the silica layer thickness by SEM (Table I).

The variations of x^2 as a function of time for $1000 < T < 1400$ °C (Fig. 1b) appear to obey a linear law and can be expressed by the equation

$$x^2 - x_0^2 = K_D\, t \quad (2)$$

where x_0 is a constant taking into account the occurrence of a silica layer which was formed during the transient regime (heating period from room temperature to T_0) prior to the isothermal treatment at T_0. The values of both x_0 and K_D are listed in Table II. It thus appears that the kinetics of oxidation of the ex-PCSZ-II Si-C-N-O filament obey a parabolic law and are diffusion-controlled.

The thermal variations of the kinetic constant K_D are shown in Fig. 2 in an Arrhenius plot and observed

TABLE I Validation of calculation procedure used to derive the thickness of the SiO_2-layer from $\Delta m/m_o$, from SEM direct measurements

	Oxidation treatment		
	200 h 1000 °C	50 h (1200 °C)	20 h (1400 °C)
Calculated SiO_2 layer thickness (nm)	527	782	1128
Measured SiO_2 layer thickness (nm)	600	800	1000

TABLE II Values of parabolic diffusion constant K_D and equivalent initial thickness at $t = 0$, x_o, for various oxidation test temperatures

	T(°C)			
	1000	1100	1200	1400
x_o (nm)	11	18	41	96
K_D ($nm^2\ s^{-1}$)	0.37	1	3.05	14.8

to obey the equation.

$$K_D = K_o \exp(-E_a/RT) \quad (3)$$

where K_o, the so-called pre-exponential constant, is equal to $3 \times 10^6\ nm^2\ s^{-1}$; E_a, the apparent activation energy, is equal to 170 kJ mol^{-1} and R is the ideal gas constant.

3.2. Failure surface of the filaments

Two SEM micrographs of the surfaces of oxidized filaments which failed under tensile loading at room temperature are shown in Fig. 3. The filament which has been maintained in dry oxygen for 200 h at 1000 °C exhibits after failure the typical surface of a brittle material and appears to be coated with a smooth layer of silica with a thickness of about 0.6 μm. Conversely, the filament which has been treated 20 h at 1400 °C, exhibits a rough and cracked silica layer with a thickness of about 1 μm.

3.3. Structure and composition of the oxide scale

TEM–EELS analyses were performed on cross-section thin foils of Si–C–N–O filaments (which had been treated for 20 h in dry oxygen at 1400 °C), prepared by ultramicrotomy according to a technique described by Maniette and Oberlin [22]. One of the TEM images taken in the bright-field (BF) mode is shown in Fig. 4a. Three different zones (referred to as zones 1, 2 and 3) are clearly apparent. The external zone 3, with a mean thickness of about 1 μm, was assigned to α-cristobalite on the basis of its selective-area diffraction (SAD) pattern. It has been observed that α-cristobalite has a tendency to become amorphous under the electron beam, as already reported by Maniette and Oberlin [22] for ex-PCS fibres. The internal zone 1 is amorphous (Fig. 4b) and was assigned to part of the non-oxidized Si–C–N–O filament. Finally, the intermediate zone 2, with a thickness of about 50 nm, was also observed to consist of an amorphous material (Fig. 4c).

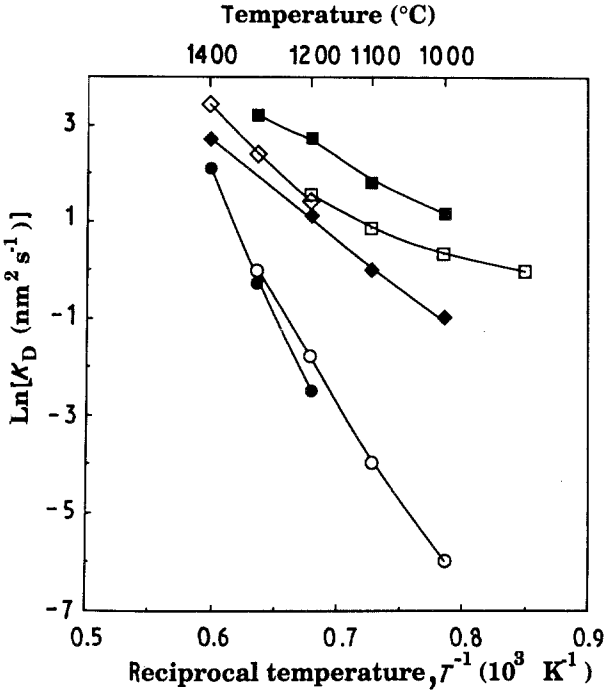

Figure 2 Arrhenius plots showing the thermal variations of the kinetic parabolic constants K_D for the oxidation of the ex-PCSZ-II Si–C–N–O filaments and various Si-based ceramics: (⊡) Si–C–O ex-PCS fibres [16], (●) bulk Si_3N_4 [28], (■) silicon single crystal (1 1 1) [24], (○) CVD Si_3N_4 [24], (◇) HP SiC [26], (◆) present work.

An elemental analysis was performed by EELS in the three different zones. The EELS spectra are shown in Fig. 5. The external zone 3, previously identified as silica, contains only silicon and oxygen (no nitrogen or carbon were detected in significant amounts), the O/Si ratio being 2.3, i.e. close to that characterizing pure silica. Furthermore, no significant concentration gradient was observed across the silica scale. The intermediate amorphous zone 2 contains carbon and it was tentatively identified as an infiltration of the resin which was used to embed the filament prior to ultramicrotomy (as supported by the fact that the α-cristobalite scale formed at 1400° C is cracked and partly debonded from the filament after cooling at room temperature, as shown in Fig. 3b). Finally, quantitative EELS analysis performed in zone 1 (corresponding to the non-oxidized ex-PCSZ-II Si–C–N–O filament) led to the overall chemical formula $SiC_{0.8}N_{0.44}O_{0.6}$, which is in rather good agreement with that established from the EPMA data, i.e. $SiC_{0.77}N_{0.39}O_{0.6}$ as reported in part III [18].

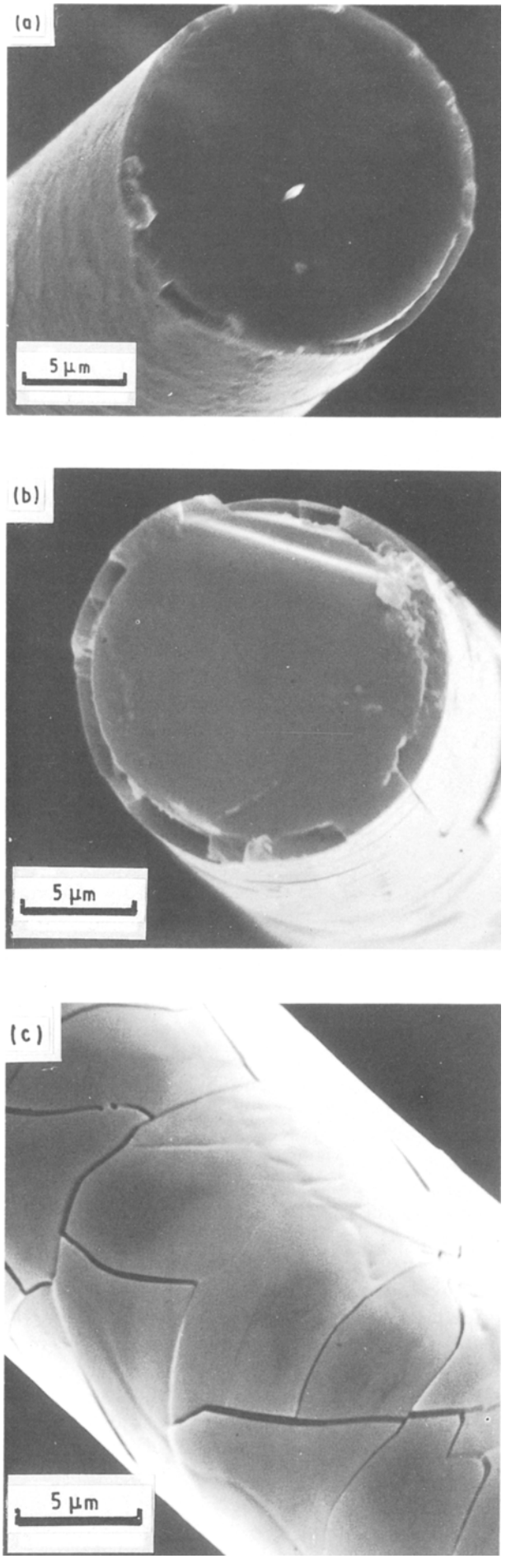

Figure 3 SEM micrographs of ex-PCSZ-II Si–C–N–O filaments after oxidation treatments in dry oxygen (P = 100 kPa, Q = 1 l h^{-1}) (a) 200 h at 1000 °C, (b) and (c) 20 h at 1400 °C.

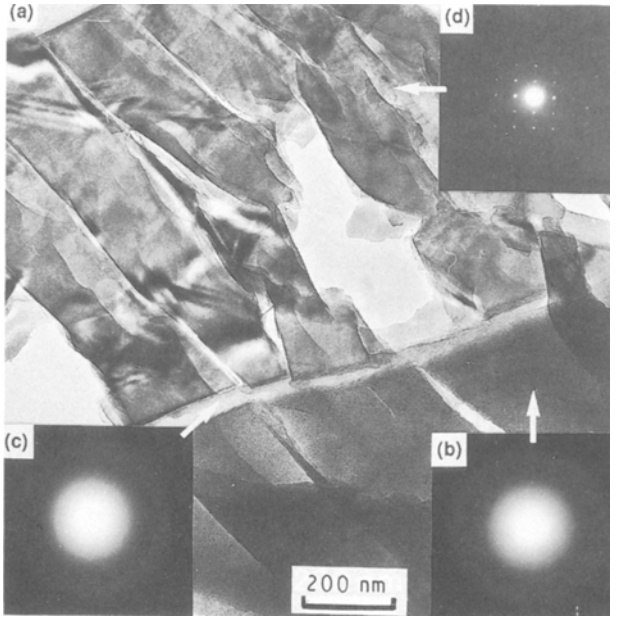

Figure 4 TEM analysis, near the external surface, of an ex-PCSZ-II, Si–C–N–O filament after oxidation treatment of 20 h at 1400 °C in dry oxygen: (a) bright-field image; (b, c, d) SAD patterns of zones 1, 2 and 3, respectively.

4. Discussion

4.1. Chemical species involved in the oxidation of ex-PCSZ-II Si–C–N–O filaments in dry oxygen

The analytical data which have been presented in section 3 clearly show that the oxidation of ex-PCSZ-II Si–C–N–O filaments results mainly in the growth of a silica layer at the filament surface whose kinetics is controlled by diffusion phenomena. The silica scale is amorphous for oxidation tests performed at low temperatures (e.g. T_o = 1000 °C) whereas it consists of α-cristobalite at high temperatures (e.g. T_o = 1400 °C). Conversely the oxidation mechanisms remain a matter of speculation owing to (i) the limited amount of experimental data and (ii) the complexity of the material (the filaments have an amorphous character and their chemical composition involves five elements and is close to the overall formula $SiC_{0.8}N_{0.4}O_{0.6}(H)$). However, it is thought that they might have common features with the oxidation mechanisms of different related materials, such as silicon, silicon carbide and silicon nitride, which have been the subject of many detailed analyses [23, 27].

It is generally accepted that the important step, from a kinetic point of view, in the oxidation of silicon by oxygen is the diffusion of oxygen through the silica layer involving molecular species at T_o < 1400 °C and ionic species at T_o > 1400 °C [23,24]. In the oxidation of silicon carbide, two opposite diffusion fluxes are present in the silica scale: (i) a flux of oxygen, as already mentioned for silicon, and (ii) a flux of carbon oxides (i.e. CO and to a less extent CO_2) [25]. Finally, the oxidation of silicon nitride also involves two opposite diffusion fluxes: a flux of oxygen and a flux of nitrogen (as molecular species) [26, 27].

Furthermore, hydrogen is present in small amounts (i.e. ~2 at %) in ex-PCSZ-II Si–C–N–O filaments and

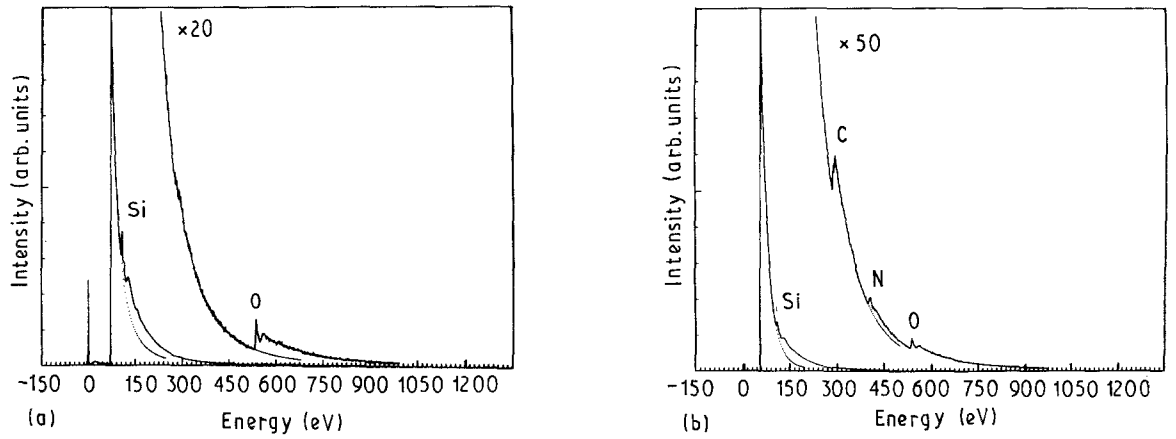

Figure 5 EELS spectra of the different zones shown in the TEM BF image of Fig. 4: (a) silica scale (zone 3) and (b) non-oxidized ex-PCSZ-II Si–C–N–O filament (zone 1).

might play a role in the oxidation process [18]. It could be responsible for the formation of OH species whose occurrence in silica would decrease the viscosity of the oxide scale and thus favour the permeation of molecular gaseous species [28]. It has also been mentioned that hydrogen enhances the formation of NO during the oxidation of Si_3N_4 by an H_2O–O_2 mixture [24].

On the basis of the various oxidation mechanisms previously reported for silicon, SiC and Si_3N_4, the oxidation of ex-PCSZ-II Si–C–N–O filaments might involve, in a similar manner, two opposite diffusion fluxes, as shown schematically in Fig. 6: (i) a flux of reactant (molecular oxygen or /and O^{2-} ions) and (ii) a complex flux of products including mainly carbon oxides (CO and to a less extent CO_2) and nitrogen (as molecular N_2 species or/and to a less extent NO species) as well as small amounts of hydrogen-containing species (H_2, OH^- or H_2O).

The local TEM–EELS analysis reported in section 3 (as well as Auger electron spectroscopy data) does not support the occurrence of an intermediate phase between the silica layer and the Si–C–N–O filament, at least at a scale larger than about 10 nm. This result is in opposition with a conclusion drawn by Du *et al.* [27] according to which a ternary material Si_2N_2O is formed, as a thin interphase, during the oxidation of Si_3N_4 by oxygen. However, the occurrence of a thin intermediate phase (with a subnanometre scale) between SiO_2 and Si–C–N–O filament is not to be strictly excluded even if it has not yet been experimentally established (owing to pollution of the interface by the resin used to embed the filament).

4.2. Morphology of the silica scale

As already mentioned, the silica scale resulting from the oxidation of ex-PCSZ-II filaments in dry oxygen is amorphous for $T_o \sim 1000\,^\circ C$ and crystalline for $T_o \sim 1400\,^\circ C$ in agreement with the data reported previously by Filipuzzi and Naslain [16] in their study of the oxidation of ex-PCS Si–C–O fibres in dry oxygen [16] and, more generally, with the data published on the oxidation of bulk SiC and Si_3N_4 ceramics [25, 26, 29, 30]. The amorphization effect of the

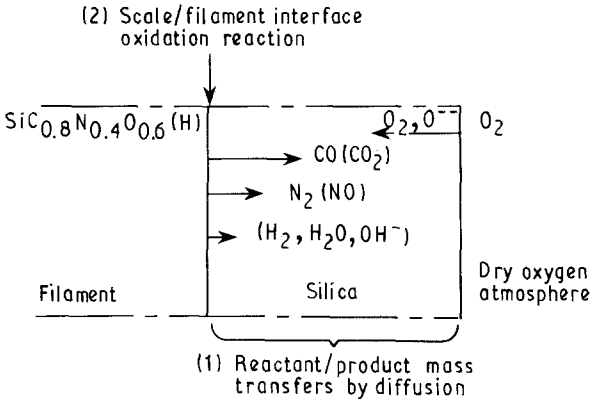

Figure 6 Tentative modelling of the oxidation of an ex-PCSZ-II Si–C–N–O filament in dry oxygen showing the mass transfers of reactant/products across the silica scale and the oxidation reaction taking place at the scale–filament interface (schematic).

electron beam on the cristobalite scale, observed during the TEM analyses, has been also mentioned by Maniette and Oberlin [22] for silica grown on ex-PCS Si–C–O fibres.

The surface of the silica scale grown at 1400 °C on the filaments is rough and contains microcracks, in contrast with that of the filaments treated at 1000 °C which is smooth and crack-free, as shown in Fig. 3. This difference could be assigned to (i) the well-known effect of the volume change occurring at the β–α transition of cristobalite upon cooling (at about 270 °C) and (ii) a coefficient of thermal expansion (CTE) mismatch between the cristobalite layer and the filament. Conversely, it does not seem that the volume change related to the Si–C–N–O/SiO_2 conversion could explain the microcracking phenomenon observed in the cristobalite scale after an oxidation test at 1400 °C (Fig. 3b). If it was the case, the microcracks would have been formed at high temperatures and have favoured the diffusion of oxygen (via the gas phase) towards the filament surface. Under such conditions, the filament oxidation would have been pronounced locally near the scale microcrack ends, a feature which has not been observed here in opposition to what has been reported for the oxidation of ex-PCS Si–C–O fibres (Nicalon fibres from Nippon Carbon) [16]. This difference of behaviour between ex-PCS Si–C–O and ex-PCSZ Si–C–N–O fibres could be

TABLE III Values of the Pilling–Bedworth coefficient Δ and the conversion factor F_R, calculated for various exorganosilicon fibres ($d_{SiO_2} = 2.22\ g\,cm^{-3}$ for all calculations) according to Equations 4 and A10

	Si–C–N–O cured at 140 °C (present work and [17])	Si–C–N–O cured at 190 °C (present work and [17, 18])	Si–C radiation-cured [13]	Si–C–O oxygen-cured [16]
Composition	$SiC_{0.9}N_{0.4}O_{0.2}$	$SiC_{0.78}N_{0.39}O_{0.61}$	$SiC^{a}_{1.3}$	$SiC_{1.2}O_{0.4}$
Silicon mass concentration, C_{Si}	0.56	0.53	0.64[a]	0.57
Fibre diameter, $2r(10^3$ nm)	18.5	20	15	15
Density ($g\,cm^{-3}$)	2.46	2.45	2.7	2.55
Pilling–Bedworth coefficient, Δ	1.33	1.26	1.68	1.41
Conversion factor, F_R ($\times 10^3$)	32	44	22	32

[a] Estimated.

explained taking into account the respective values of the so-called coefficient of Pilling and Bedworth [29, 31] Δ.

In the oxidation of silicon-based ceramic material, Δ is defined as the volume of silica formed per volume of ceramic consumed. As shown in the Appendix, it can be expressed according to the equation

$$\Delta = \frac{M_{SiO_2}}{M_{Si}}\left(\frac{d}{d_{SiO_2}}\right)C_{Si} \quad (4)$$

where M_{SiO_2} and M_{Si} are the molar masses of silica and silicon, d and d_{SiO_2} the densities of the ceramic and silica, respectively, and C_{Si} the mass concentration in silicon of the ceramic material. When $\Delta > 1$, oxidation of the ceramic yields an oxide scale which has the capability of covering the ceramic substrate in a continuous manner. It appears from Equation 4 that ceramics with a high silicon concentration and density are characterized by high Δ values (e.g. $\Delta = 2.24$ and 2.18 for pure silicon and silicon carbide, respectively). Furthermore, since silica is formed continuously at the scale–substrate interface (Fig. 6), the mechanical stress level will be more significant when Δ is high unless the stresses can be properly released (e.g. by viscous flow). The values of Δ, calculated according to Equation 4 for various ex-organosilicon fibres, are listed in Table III. High values of Δ are thought to favour the occurrence of mechanical stresses and thus that of cracks during the growth of thick and rigid oxide scales: microcracks and enhanced oxidation at the crack ends have been reported for ex-PCS Si–C–O fibres whose Δ value is 1.41, as already mentioned [16]. Conversely, values of Δ close to unity are thought to induce lower mechanical stress levels in the scale; this might be the case for the ex-PCSZ-II Si–C–N–O filaments studied here, whose Δ value is only 1.26, the microcracks observed after an oxidation test at 1400 °C being formed upon cooling as the result of other phenomena (i.e. α–β cristobalite transition and/or CTE mismatch).

4.3. Kinetics of growth of the silica scale

As shown in section 2, the kinetics of growth of the silica layer on ex-PCSZ-II Si–C–N–O filaments in dry oxygen obeys a parabolic law. The observed overall weight increase $\Delta m/m_o$ is the result of two opposite phenomena: (i) the weight increase related to the oxidation of silicon and (ii) the weight loss due to the release of gaseous species (mainly CO and N_2). The overall reaction can be expressed by the equation

$$SiC_{0.8}N_{0.4}O_{0.6} + 1.1O_2 \rightarrow SiO_2 + 0.8CO + 0.2N_2 \quad (5)$$

in which hydrogen, known to be present in the filament in small amounts (≈ 2 at %), is not taken into account. This equation should be compared with those characterizing the oxidation of related Si-based materials, i.e. ex-PCS Si–C–O Nicalon fibres, silicon carbide, silicon and silicon nitride:

$$SiC_{1.2}O_{0.4} + 1.4O_2 \rightarrow SiO_2 + 1.2CO \quad (6)$$

$$SiC + 1.5O_2 \rightarrow SiO_2 + CO \quad (7)$$

$$Si + O_2 \rightarrow SiO_2 \quad (8)$$

$$\frac{1}{3}Si_3N_4 + O_2 \rightarrow SiO_2 + \frac{2}{3}N_2 \quad (9)$$

The values of the kinetic parabolic constant K_D (defined in Equation 2) and the apparent activation energy E_a (defined in Equation 3) are listed in Table IV for the ex-PCSZ-II Si–C–N–O filaments studied here as well as for some related Si-based materials for the purpose of comparison. The thermal variations of K_D are shown in Fig. 2.

The kinetics of growth of the silica scale which has been established in the present work for the ex-PCSZ-II Si–C–N–O filaments exhibits two important features with respect to those previously published for the related ex-PCS Si–C–O fibres [16] : (i) the parabolic rate constant K_D at a given temperature is lower, the ratio between the respective rate constants, K_D(Si-C-O)/K_D(Si–C–N–O), being larger at low temperatures (e.g. its value is 4 at 1000 °C and only 1.5 at 1200 °C) (Table IV); and (ii) the parabolic growth law of the silica is still obeyed up to 1400 °C for the ex-PCS II Si–C–N–O filaments whereas this is no longer true beyond 1200 °C for the ex-PCS Si–C–O Nicalon fibres, as previously reported [16]. This latter feature is thought to be related to the fact that the filaments studied in the present work are stable up to 1400 °C from a microstructural point of view, whereas the ex-PCS Si–C–O filaments are known to undergo beyond about 1200 °C a decomposition–crystallization process [11, 30]. As shown in Fig. 3, the thickness of the silica scale formed in dry oxygen at high temperatures is significantly higher for the ex-PCS Si–C–O filaments with respect to the ex-PCSZ-II Si–C–N–O

TABLE IV Variations of the parabolic kinetic constant K_D ($nm^2\ s^{-1}$) as a function of oxidation test temperature for various Si-based ceramic materials

Material	Sample	K_D ($nm^2\ s^{-1}$)							
		900 °C	1000 °C	1100 °C	1200 °C	1300 °C	1400 °C	E_a (kJ mol^{-1})	Ref.
Silicon	Single crystal (111)		3.2	6.3	15.8	25	37	111	[24]
Silicon carbide	HP SiC				4.1	11	30	200	[26]
Silicon nitride	CVD Si_3N_4				0.08	0.76	8	468	[24]
Silicon nitride	CVD Si_3N_4		0.002	0.02	0.16	1		330	[28]
Si–C–O	Fibre (ex-PCS)[a]	0.96	1.38	2.31	4.75			70	[16]
Si–C–N–O (ex-PCSZ II) cured at 190 °C	Filament (amorphous)		0.37	1	3.05		14.8	170	Present work

[a] Nicalon fibres (grade NLM 202) from Nippon Carbon.

filaments, owing to the various degradation phenomena which take place in the former and which are thought to enhance the oxygen diffusion (e.g. the scale microcracking discussed in Section 4.2). As an example, the mean thickness of the silica layer observed after an oxidation test of 10 h at 1400 °C was observed to be 3 μm for an ex-PCS Si–C–O fibre (Nicalon grade NLM 202) but only 0.7 μm for ex-PCSZ-II Si–C–N–O filaments.

As shown in Fig. 2, the growth rate of the silica is thermally activated, the variations of $\ln K_D$ as a function of the reciprocal temperature being linear within the whole temperature range which has been studied. This feature, together with the parabolic character of the kinetics of growth of the silica layer, supports the assumption that the rate-limiting step in the growth of the oxide scale is a diffusion mechanism. The value of the related apparent activation energy, i.e. $E_a = 170\ kJ\ mol^{-1}$, is significantly higher than that reported previously for ex-PCS Si–C–O Nicalon fibres i.e. $70\ kJ\ mol^{-1}$ [16]. It is worthy of note that the apparent activation energy reported for Si_3N_4 (from 330 to 468 $kJ\ mol^{-1}$) [24,30] is also higher than that measured for SiC (from 200 to 300 $kJ\ mol^{-1}$) [27]. Thus, it is thought that these coherent differences could be related to some effect of nitrogen on the mass transfers of the oxygen-containing species (not to say oxygen itself) through silica (Fig. 6) which would be particularly effective at low temperatures (Fig. 2). The occurrence of some nitrogen in the silica glass formed at low temperatures might increase the viscosity of the medium through which molecular oxygen has to diffuse. Furthermore, the nitrogen flux through silica might also lower the permeation rate of molecular oxygen in the opposite direction (especially if the same sites are involved in both cases), as already suggested by Clarke [30] for the oxidation of Si_3N_4. Conversely, we have not been able to establish the occurrence of a thin layer of Si_2N_2O at the Si–C–N–O/SiO_2 interface in opposition to what has been reported by Du *et al.* [27] for the oxidation of Si_3N_4. This latter difference could be related to the fact that the ex-PCSZ-II Si–C–N–O filament material already contains a large amount of oxygen (thus rendering unnecessary the formation of the Si_2N_2O phase at the interface with silica) or/and artefacts during the TEM analysis, as already mentioned in section 3.3.

The role played by hydrogen, which is known to be present in small amounts in most ex-organosilicon fibres, in the kinetics of growth of the silica layer has been discussed previously for the ex-PCS Si–C–O Nicalon fibres [16]. It has been suggested that H_2 or/and H_2O formed at the filament–silica interface could yield Si–H and Si–OH bonds whose occurrence in silica glass could be responsible to some extent for the low value of the apparent activation energy, i.e. $70\ kJ\ mol^{-1}$. Different assumptions have been made to justify the role played by H_2/H_2O including a lowering of the silica glass viscosity [28]. A similar effect could be present in the ex-PCSZ-II Si–C–N–O filaments (whose hydrogen concentration is of the same order of magnitude); however, this subject remains a matter of speculation and would require more experimental support.

Carbon monoxide is formed according to Equations 5 and 6 in about the same amounts for ex-PCS Si–C–O and ex-PCSZ-II Si–C–N–O filaments. Its mass transfer of CO by diffusion across the silica layer is not thought to be the rate-limiting step at low temperatures, as previously suggested by Du *et al.* [27] in their study of the oxidation of Si–C ceramics.

It appears from Fig. 2 that the kinetic parabolic rate constants K_D tend towards values which are close together for tests performed at very high temperatures (e.g. 1400 °C). Under such conditions, the mass transfer across the silica layer might be rate-controlled by

the diffusion of O^{2-} ions. Conversely, at low temperature (e.g. 1000 °C) the values of K_D are very different from one another. If one assumes that the rate-controlling step is the permeation of molecular oxygen across silica, it can be understood that the kinetics of the process are dependent on the heteroatoms which are present and thus are different for the various materials.

5. Conclusion

The oxidation of ex-PCSZ-II Si–C–N–O model filaments in dry oxygen ($P = 100$ kPa) results in the growth of a silica scale and simultaneously the release of carbon oxides and nitrogen. Within the temperature range 1000–1400 °C, the kinetics of growth of the silica scale remain parabolic, the kinetic parabolic constant K_D being thermally activated with an apparent activation energy E_a of 170 kJ mol^{-1}. These features suggest that the rate-limiting step is a diffusion-controlled mechanism (which might be the mass transfer of oxygen across the silica layer). The oxidation of the ex-PCSZ-II Si–C–N–O filaments thus exhibits common features with those of SiC and Si_3N_4.

With respect to the oxidation of the related ex-PCS oxygen-cured Si–C–O fibres, that of the model filaments derived from PCSZ precursors exhibits three major differences: (i) at a given temperature, the thickness of the silica layer is lower for the ex-PCSZ filaments (i.e. their oxidation resistance is higher), (ii) the kinetics of growth of the silica scale remains parabolic for $1000 < T_o < 1400$ °C whereas this is no longer true for the ex-PCS fibres beyond about 1200 °C, and (iii) the temperature dependence of the parabolic rate constant is higher for the ex-PCSZ filaments.

It thus appears that the ex-PCSZ-II filaments have a better behaviour in oxidizing atmospheres than their ex-PCS counterparts.

Appendix

A1. The Pilling–Bedworth factor

It is assumed that during the oxidation of a silicon-based ceramic material all the silicon atoms are converted into silica, the other atoms being released as gaseous species. The Pilling–Bedworth factor Δ is defined as the ratio between the silica volume formed, V, and the volume of ceramic material which has been oxidized, V_o.

Let m_o, m and C_{Si} be the mass of ceramic material oxidized, the mass of silica formed and the silicon mass concentration of the starting material, respectively; then

$$V_o = \frac{m_o}{d} \tag{A1}$$

$$V = \frac{m}{d_{SiO_2}} = \frac{m_o C_{Si}}{d_{SiO_2}}\left(\frac{M_{SiO_2}}{M_{Si}}\right) \tag{A2}$$

where d is the density of the ceramic material, d_{SiO_2} that of silica, M_{SiO_2} the molar mass of the ceramic material and M_{Si} that of silicon. Then

$$\Delta = \frac{V}{V_o} = \frac{M_{SiO_2}}{M_{Si}}\left(\frac{d}{d_{SiO_2}}\right)C_{Si} \tag{A3}$$

A2. Assumptions

For the derivation of the conversion factor F_C used to calculate the thickness of the silica layer x from the measured weight change due to oxidation $\Delta m/m_o$, the following assumptions are made : (i) the ceramic material has no porosity (i.e. the surface seen by oxygen is the external surface), (ii) the density of the oxide scale is constant, and (iii) the external surface is assumed to be planar (since the oxide scale thickness is small with respect to the filament radius).

The thickness e_o of the parallelepiped body having the same volume V_o and surface S_o as the cylindrical filament (neglecting the lateral surfaces) is defined according to the equation

$$e_o = \frac{V_o}{S_o} = \frac{\pi r^2 l}{2\pi r l} = \frac{r}{2} \tag{A4}$$

where r is the radius of the filament and l its length. In the following and as shown in Fig. A1, the calculations will be done on the equivalent parallelepiped volume, assuming that only one face is oxidized and its surface remains constant and equal to S_o.

A3. Complete oxidation of the ceramic body

The equivalent parallelepiped body has an initial mass which is $m_o = (r/2)\, S_o d$. If the oxidation treatment is long enough (i.e. for $t = t_f$), it will yield quantitatively a mass of silica m given by

$$m = m_o C_{Si}\left(\frac{M_{SiO_2}}{M_{Si}}\right) \tag{A5}$$

In the oxidation process, it is assumed that all the silicon present initially in the ceramic body is converted into silica, the other elements being either integrated into the silica scale (e.g. oxygen) or released as gaseous species (i.e. C as CO or CO_2 and N as N_2). The initial volume of ceramic material V_o and the final volume of silica are those given by Equations A1 and A2, respectively.

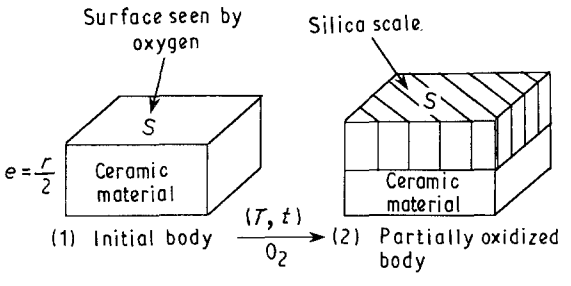

Figure A1 Parallelepiped body equivalent to the actual cylindrical filament.

The overall mass change Δm_f corresponding to the quantitative conversion of the initial mass m_0 of ceramic material into silica is given by

$$\Delta m_f = m_o\left(\frac{M_{SiO_2}}{M_{Si}}C_{Si} - 1\right) \quad (A6)$$

It is worthy of note that a transition between an overall weight increase to an overall weight loss occurs when $C_{Si} = 46.6\%$, assuming, as mentioned above, that the elements other than silicon (e.g. C and N) are released as gaseous species. Obviously, if the ceramic material contains other elements forming condensed oxides (e.g. titanium, known to be present in some fibres (Tyranno fibres from Ube), these elements would have to be treated as silicon.

Finally, the overall thickness e_f of the parallelepiped body when quantitatively converted into silica is given by

$$e_f = \frac{V}{S_o} = \frac{M_o C_{Si}}{d_{SiO_2}}\left(\frac{M_{SiO_2}}{M_{Si}}\right)\frac{1}{S_o} \quad (A7)$$

or, replacing m_o by $(r/2)\, S_o d$,

$$e_f = \frac{1}{2}\left(\frac{M_{SiO_2}}{M_{Si}}\right)\frac{d}{d_{SiO_2}}C_{Si}r \quad (A7')$$

or, by combining Equations (A7′) and (A3)

$$e_f = \frac{1}{2}\Delta r \quad (A7'')$$

A4. Partial oxidation of the ceramic body

During the oxidation tests which have been performed in the present work, only a small fraction of the initial filament is converted into silica. This is shown in Fig. A2 for the equivalent parallelepiped body.

At an intermediate time t, it is assumed that the thickness x of the silica scale is proportional to the actual weight increase Δm, which can be written as

$$\frac{x}{\Delta m} = \frac{e_f}{\Delta m_f} \quad (A8)$$

Thus the thickness of the oxide scale at time t is given by

$$x = \frac{\Delta m}{\Delta m_f}e_f \quad (A8')$$

Replacing e_f and Δm_f by their expressions given by Equations (A7′) and (A6), Equation (A8′) can be rewritten as

$$\frac{x}{r} = \frac{1}{2}\left(\frac{M_{SiO_2}C_{Si}}{M_{SiO_2}C_{Si} - M_{Si}}\right)\left(\frac{d}{d_{SiO_2}}\right)\left(\frac{\Delta m}{m_o}\right) \quad (A9)$$

Defining the conversion factor F_C as

$$F_C = \frac{1}{2}\left(\frac{M_{SiO_2}C_{Si}}{M_{SiO_2}C_{Si} - M_{Si}}\right)\frac{d}{d_{SiO_2}} \quad (A10)$$

Equation (A9) can be rewritten as

$$\frac{x}{r} = F_C\frac{\Delta m}{m_o} \quad (A11)$$

which has been used to calculate the values of x from the values of $\Delta m/m_o$ measured by TGA. Note that (i) F_C is a dimensionless coefficient and (ii) its value for ex-PCSZ Si–C–N–O filaments is equal to 0.04.

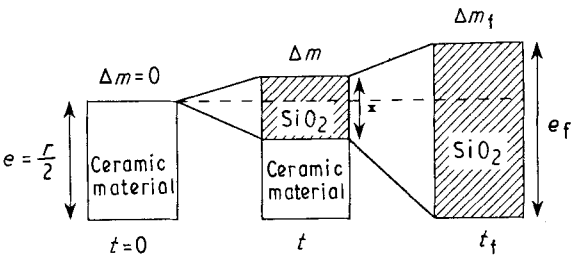

Figure A2 Growth of silica scale on the equivalent parallelepiped body from $t = 0$ to $t = t_f$.

Acknowledgements

This work has been performed within the framework of a national programme of research on ceramic organosilicon precursors supported by CNRS, DRET, RP and SEP. The authors acknowledge the contribution of M. Chambon (CUMEMSE, UB1) and J. Fourmeaux (CEMES-LOE) to the TEM–EELS analyses and that of C. Richard and J.P. Pillot (URA-35, UB1) to the preparation of the PCSZ precursors.

References

1. Y. HASEGAWA, M. IIMURA and S. YAJIMA, *J. Mater. Sci.* **15** (1980) 720.
2. Y. HASEGAWA, *ibid.* **24** (1989) 1177.
3. T. YAMAMURA, T. HURUSHIMA, M. KIMOTO, T. ISHIKAWA, M. SHIBUYA and T. IWAI, in "High Tech. Ceramics", edited by P. Vincenzini (Elsevier Science, Amsterdam, 1987) p. 737.
4. D. B. FISHBACH, P. M. LEMOINE and G. V. YEN, *J. Mater. Sci.* **23** (1988) 987.
5. B. G. PENN, F. E. LEDBETTER III, J. M. CLEMONS and J. G. DANIELS, *J. Appl. Polym. Sci.* **27** (1982) 3751.
6. G. PEREZ and O. CAIX, in Proceedings of 4th European Conference on Composite Materials (ECCM 4), edited by J. Füller, G. Gruninger, K. Schulte, A. R. Bunsell and A. Massiah (Elsevier Applied Science, London, 1990) p. 573.
7. R. NASLAIN, in "Introduction to Composite Materials", Vol. 2, "Metallic and Ceramic Matrix Composites", (CNRS/IMC, Bordeaux, 1985) p. 19.
8. D. C. PHILLIPS, *Compos. Sci. Technol.* **40** (1991) 1.
9. J. R. STRIFE, J. J. BRENNAN and K. M. PREWO, *Ceram. Eng. Sci. Proc.* **11** (1990) 871.
10. T. J. CLARCK, E. R. PRACK, M. I. HAIDER and L. C. SAWYER, *ibid.* **8** (1987) 717.
11. S. M. JOHNSON, R. D. BRITTAIN, R. M. LAMOREAUX and D. J. RAWCLIFFE, *J. Amer. Ceram. Soc.* **71** (3) (1988) 132.
12. K. L. LUTHRA, *ibid.* **69** (10) (1986) 231.
13. K. OKAMURA, M. SATO, T. SEGUCHI and S. KAWANISHI, in "Controlled Interphases in Composite Materials", edited by Hatsuo Ishida, (Elsevier Science, 1990) p. 209.
14. D. MOCAER, R. PAILLER, R. NASLAIN, C. RICHARD, J. P. PILLOT, J. DUNOGUES, M. CHAMBON, M. LAHAYE and C. DARNEZ, *J. Mater. Sci.* **28** (1993) 3049.
15. R. WARREN and C. H. ANDERSEN, *Composites* **15** (2) (1984) 101.
16. L. FILIPUZZI and R. NASLAIN, in Proceedings of 7th CIMTEC World Ceramic Congress and Satellite Symposium, Montecatini Terme, Italy, 1990.

17. D. MOCAER, R. PAILLER, R. NASLAIN, C. RICHARD, J. P. PILLOT and J. DUNOGUES, *J. Mater. Sci.* **28** (1993) 2615.
18. D. MOCAER, R. PAILLER, R. NASLAIN, C. RICHARD, J. P. PILLOT, J. DUNOGUES, O. DELVERDIER and M. MONTHIOUX, *ibid.* **28** (1993) 2632.
19. E. BACQUE, J. P. PILLOT, J. DUNOGUES and P. OLRY, European Patent 296 028 (1988).
20. D. MOCAER, R. PAILLER, R. NASLAIN, C. RICHARD, J. P. PILLOT, J. DUNOGUES, F. TAULLELE and V. GERARDIN, *J. Mater. Sci.* **28** (1993) 2639.
21. W. L. VAUGHN and H. G. MAAHS, *J. Amer. Ceram. Soc.* **73** (1990) 3361.
22. Y. MANIETTE and A. OBERLIN, *J. Mater. Sci.* **24** (1989) 3361.
23. R. H. DOREMUS and A. SZEWCZYK, *ibid.* **22** (1987) 2887.
24. D. J. CHOI, D. B. FISCHBACH and W. D. SCOTT, *J. Amer. Ceram. Soc.* **72** (1989) 1118.
25. J. A. COSTELLO and R. E. TRESSLER, *ibid.* **69** (1986) 674.
26. W. C. TRIPP and H. C. GRAHAM, *J. Amer. Ceram. Soc.* **59**, (1976) 399.
27. H. DU, R. E. TRESSLER, K. E. SPEAR and C. G. PANTANO, *J. Electrochem. Soc.* **136** (1989) 1527.
28. H. DU, R. E. TRESSLER and K. E. SPEAR, *ibid.* **136** (1989) 3210.
29. N. G. PILLING and R. E. BEDWORTH *J. Inst. Met.* **29** (1923) 529.
30. D. R. CLARKE, in "Progress in Nitrogen Ceramics", edited by F. L. Riley (Nijhoff, Boston, 1983) p. 421.
31. G. H. SCHIROKY, *Adv. Ceram. Mater.* **2** (2) (1987) 137.

Received 20 July
and accepted 11 August 1992